Mathematical Models and Methods in Applied Sciences

Finite difference/finite element method for two-dimensional time and space fractional Bloch-Torrey equations with variable coefficients on irregular convex domains

Tao Xu
School of Mathematics and Sciences, Beihang University
Beijing 100191, China
xutao0828@126.com

Fawang Liu*
School of Mathematical Sciences, Queensland University of Technology
QLD 4001, Australia
College of Mathematics and Computer Science, Fuzhou University
Fujian 350116, China
Corresponding author: f.liu@qut.edu.au

Shujuan Lü
School of Mathematics and Sciences, Beihang University
Beijing 100191, China
lsj@buaa.edu.cn

Vo Anh
Engineering and Technology, Swinburne University of Technology
PO'Box 218, HaWthorn, VIC 31ZZ,.Australia
v.anh@qut.edu.au

Received (Day Month Year)
Revised (Day Month Year)
Communicated by (xxxxxxxxxx)

In magnetic resonance imaging of the human brain, the diffusion process of tissue water is considered in the complex tissue environment of cells, membranes and connective tissue. Models based on fractional order Bloch-Torrey equations can provide a new insights into further investigations of tissue structures and the microenvironment.

In this paper, we consider new two-dimensional multi-term time and space fractional Bloch-Torrey equations with variable coefficients on irregular convex domains, which involves the Caputo time fractional derivative and the Riemann-Liouville space fractional derivative. An unstructured-mesh Galerkin finite element method is used to discretise the spatial fractional derivative, while for each time fractional derivative we use a novel $L1$ scheme on a temporal graded mesh. The stability and convergence of the fully discrete scheme are proved. Numerical examples are given to verify the efficiency of our method.

Keywords: Bloch-Torrey equations; Galerkin finite element method; Irregular domains;

Variable coefficients; Graded mesh.

AMS Subject Classification: 65M06, 65M60, 65M12, 26A33

1. Introduction

Fractional calculus has attracted considerable interest in recent years because of their ability to model temporal memory, non-local properties, anomalous diffusion and spatial heterogeneity. Over the past two decades, fractional differential equations have been used in physics, biology, chemistry, hydrology, finance, and the related theory of fractional calculus is growing rapidly.[1,5,6,17,21,24,29,30,32,33]

Fractional diffusion equations (FDEs) form one of the most important classes of mathematical models for description of the anomalous diffusion transport process.[20,23,26–28,49] Recently, some authors have developed a new class of fractional diffusion models called the time and space fractional Bloch-Torrey equations to accommodate sub- and super-diffusion processes in biological tissues. It has been shown that these models are more appropriate than the classical diffusion models to fit experimental data. The fractional version of the Bloch-Torrey equation is given by

$$\sigma^{\alpha-1}\,{}_0^C D_t^\alpha M_{xy}(\mathbf{r},t) = \lambda M_{xy}(\mathbf{r},t) + D\mu^{\gamma-2}\mathbf{R}^\gamma M_{xy}(\mathbf{r},t), \tag{1.1}$$

where $M_{xy}(\mathbf{r},t)$ is the transverse component of the magnetisation: $M_{xy}(\mathbf{r},t) = M_x(\mathbf{r},t) + iM_y(\mathbf{r},t)$ with $i=\sqrt{-1}$, $\lambda = -i\rho(\mathbf{r}\cdot\mathbf{G})$, ρ is the gyromagnetic ratio, $\mathbf{G}$ is the magnetic field gradient, $\mathbf{r}=(x,y)$ is the coordinate, D is the diffusion coefficient, σ and μ are parameters needed to preserve the units, ${}_0^C D_t^\alpha$ is the Caputo time fractional derivative of order $\alpha(0<\alpha\le 1)$ defined as

$${}_0^C D_t^\alpha u(x,y,t) = \frac{1}{\Gamma(1-\alpha)}\int_0^t \frac{\partial u(x,y,s)}{\partial s}(t-s)^{-\alpha}\mathrm{d}s,$$

and the γ -order $(1<\gamma\le 2)$ two-dimensional Riesz fractional order operator $\mathbf{R}^\gamma = \frac{\partial^\gamma}{\partial|x|^\gamma} + \frac{\partial^\gamma}{\partial|y|^\gamma}$ with $\frac{\partial^\gamma}{\partial|x|^\gamma}$(similar for $\frac{\partial^\gamma}{\partial|y|^\gamma}$) being defined as

$$\frac{\partial^\gamma}{\partial|x|^\gamma} = -c_\gamma({}_aD_x^\gamma + {}_xD_b^\gamma)u(x,y,t),$$

where $a<x<b$, $c_\gamma = \frac{1}{2\cos(\pi\gamma/2)}$ $(\gamma\neq 1)$ and

$${}_aD_x^\gamma u(x,y,t) = \frac{1}{\Gamma(2-\gamma)}\frac{\partial^2}{\partial x^2}\int_a^x \frac{u(x,y,t)}{(x-s)^{\gamma-1}}\mathrm{d}s,$$
$${}_xD_b^\gamma u(x,y,t) = \frac{(-1)^2}{\Gamma(2-\gamma)}\frac{\partial^2}{\partial x^2}\int_x^b \frac{u(x,y,t)}{(s-x)^{\gamma-1}}\mathrm{d}s.$$

These models have been successfully applied to analyse diffusion images of human brain tissue and presents a way to simulate diffusion in the ventricles.[2,25,34–36,42,43]

However, researchers have found that the single-term time fractional derivative cannot adequately describe many complex physical or biological processes.[31] In

MRI, varying values of model parameters have been used to characterize the human brain through voxel-level fittings[34] and these parameters are associated with the tissue microstructure features, which vary on a scale much smaller than the image voxel size.[44] The existence of different fractional orders within a voxel indicate a potential use of the multi-term time fractional derivative.[34] This motivates us to extend the system (1.1) into the following coupled system involving M_x and M_y by extracting the real and imaginary parts of M_{xy} :

$$\begin{cases} P_{\alpha_1,\alpha_2,\ldots,\alpha_r}({}_0^C D_t)M_x(\mathbf{r},t) = \lambda M_y(\mathbf{r},t) + D\mu^{\gamma-2}\mathbf{R}^\gamma M_x(\mathbf{r},t), \\ P_{\alpha_1,\alpha_2,\ldots,\alpha_r}({}_0^C D_t)M_y(\mathbf{r},t) = -\lambda M_x(\mathbf{r},t) + D\mu^{\gamma-2}\mathbf{R}^\gamma M_y(\mathbf{r},t), \end{cases}$$

where $P_{\alpha_1,\alpha_2,\ldots,\alpha_r}({}_0^C D_t) = \sum_{i=1}^{r} l_i \, {}_0^C D_t^{\alpha_i}$ with the weighted coefficients $l_i \in \mathbb{R}^+$ and $0 < \alpha_r < \ldots < \alpha_2 < \alpha_1 < 1$. As in the work of Yu et al.,[43] the above equation can be equivalently transformed into the following time and space fractional differential equations to allow analysis of the numerical scheme:

$$P_{\alpha_1,\alpha_2,\ldots,\alpha_r}({}_0^C D_t)M(\mathbf{r},t) = k_\gamma\left(\frac{\partial^\gamma}{\partial|x|^\gamma} + \frac{\partial^\gamma}{\partial|y|^\gamma}\right)M(\mathbf{r},t) + f(\mathbf{r},t),$$

where M can be either M_x or M_y, and $f = \lambda M_y$ if $M = M_x$, $f = -\lambda M_x$ if $M = M_y$, $k_\gamma = D\mu^{\gamma-2}$.

In fact, the ventricles (see the blue part in Fig. 1.) are structures that contain cerebrospinal fluid and provide a cavity for its transportation in the brain. But the cavity contains the choroid plexus, which restricts and hinders diffusion leading to the potential of fast and slow diffusion processes within the cranial cavity. So the diffusion process is often heterogeneous, the diffusion coefficient may be space-dependent and can vary over the solution domain. Therefore, in this paper, we focus on the following more generalised model with variable diffusion coefficients:

$$\begin{aligned} &P_{\alpha_1,\alpha_2,\ldots,\alpha_r}({}_0^C D_t)u(x,y,t) - D_x\Big(k(x,y)D_{\theta_1}^\beta u(x,y,t)\Big) - D_y\Big(k(x,y)D_{\theta_2}^\beta u(x,y,t)\Big) \\ &= f(x,y,t), \quad (x,y,t) \in \Omega \times (0,T], \end{aligned} \tag{1.2}$$

with the initial condition

$$u(x,y,0) = \phi(x,y), \ (x,y) \in \overline{\Omega}, \tag{1.3}$$

and boundary condition

$$u(x,y,t) = 0, \ (x,y,t) \in \partial\Omega \times [0,T], \tag{1.4}$$

where $\theta_1, \theta_2 \in [0,1]$ and $D_{\theta_1}^\beta = \theta_1 \, {}_{c(y)}D_x^\beta - (1-\theta_1)_x D_{r(y)}^\beta$, $D_{\theta_2}^\beta = \theta_2 \, {}_{g(x)}D_y^\beta - (1-\theta_2) \, {}_y D_{m(x)}^\beta$, $k(x,y) > 0$ is the diffusivity coefficient satisfying the conditions in the following parts, $f(x,y,t)$ and $\phi(x,y)$ are smooth functions.

As shown in Fig. 1, the ventricles have irregular shapes in the brain, which can be represented by using irregular domains with unstructured meshes. So in this work, we consider the problem on irregular convex domains. The boundaries of the

irregular convex domain Ω are defined as: $\Omega = \{(x,y)|c(y) < x < r(y), a_1 < y < b_1\}$ or $\Omega = \{(x,y)|g(x) < y < m(x), c_1 < x < d_1\}$, where $a_1 = \min\limits_{(x,y)\in\Omega} g(x)$, $b_1 = \max\limits_{(x,y)\in\Omega} m(x)$, $c_1 = \min\limits_{(x,y)\in\Omega} c(y)$ and $d_1 = \max\limits_{(x,y)\in\Omega} r(y)$. The left and right fractional derivatives of Riemann-Liouville form of order β $(0 < \beta < 1)$ on irregular domains are defined as

$$
\begin{aligned}
{}_{c(y)}D_x^{\beta}u(x,y,t) &= \frac{1}{\Gamma(1-\beta)}\frac{\partial}{\partial x}\int_{c(y)}^{x}(x-s)^{-\beta}u(s,y,t)\mathrm{d}s,\\
{}_{x}D_{r(y)}^{\beta}u(x,y,t) &= \frac{-1}{\Gamma(1-\beta)}\frac{\partial}{\partial x}\int_{x}^{r(y)}(s-x)^{-\beta}u(s,y,t)\mathrm{d}s,\\
{}_{g(x)}D_y^{\beta}u(x,y,t) &= \frac{1}{\Gamma(1-\beta)}\frac{\partial}{\partial y}\int_{g(x)}^{y}(y-s)^{-\beta}u(x,s,t)\mathrm{d}s,\\
{}_{y}D_{m(x)}^{\beta}u(x,y,t) &= \frac{-1}{\Gamma(1-\beta)}\frac{\partial}{\partial y}\int_{y}^{m(x)}(s-y)^{-\beta}u(x,s,t)\mathrm{d}s.
\end{aligned}
$$

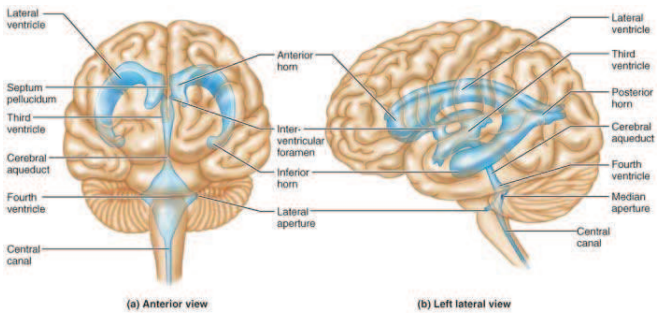

Fig. 1. Ventricles of the brain. (Source: [Marieb 2006]).

Many numerical methods have been proposed to deal with the problems involving fractional order derivatives.[24] Such as finite difference method,[21,49,50] finite volume methods,[22] the finite element method,[9,10] spectral methods,[46,51] and meshfree methods.[19] Among them, the finite element method (FEM) is an efficient numerical method widely used in engineering design and analysis. Ervin and Roop[7,8] were the first to investigate the theoretical framework for the Galerkin finite element approximation to the fractional advection-dispersion equation. Subsequently, many works have been undertaken in this area, such as.[2–4,11,12,16,18,35,45,47,48] Here, we mention some papers considering the FEM on unstructured meshes. Yang et al.[41] established the unstructured mesh FEM for the nonlinear Riesz space FDE on irregular convex domains. Fan et al. discussed the FEM for the two-dimensional time-space fractional wave equation[10] and two-dimensional multi-term time-space fractional diffusion-wave equation[9] on irregular convex domains. In,[13] Feng et al. investigated

the unstructured mesh FEM for a two-dimensional time-space Riesz FDE on irregular arbitrarily shaped convex domains and a multiply-connected domains. Liu et al.[25] presented an unstructured-mesh Galerkin FEM for the two-dimensional multi-term time-space fractional Bloch-Torrey equations on irregular convex domains. In,[42] Yang et al. proposed an unstructured mesh FEM for the three-dimensional time-space fractional Bloch-Torrey equations on irregular domains.

In this paper, we pay attention to FEM for FDEs due to its flexibility in handing problems with irregular domains.[23] Wang et al.[37] showed that the bilinear form of the Galerkin weak formulation may lose coercivity for a variable-coefficient space-fractional diffusion equation. To circumvent the difficulty, they proposed a discontinuous Petrov-Galerkin method[38,39] and indirect method[40,52] to established its well-posedness. Recently, Hao et al.[14] investigated the Galerkin approach to discretize two-sided FDEs with variable coefficients by deriving a required condition for the well-posedness of the equations, discretize the equations and provide its error estimates. We extended the ideas of[14] to two-dimensional fractional diffusion equations.

The main contributions of this work are as follows. We consider the FEM for the two-dimensional multi-term time and space fractional Bloch-Torrey equations with variable diffusivity coefficients on irregular domains. To the authors' knowledge, this topic has not been covered in the published works. For the multi-term time fractional derivative, we approximate it by the well-known L_1 scheme on a graded temporal mesh, which takes into account the weak singularity near the initial time $t = 0$ under some proper regularity and compatibility assumptions. For the space fractional derivative, we utilize FEM and unstructured triangular meshes on an irregular convex domain, which is very flexible because our considered solution domain can be arbitrarily convex and need fewer grid nodes to generate the meshes. Furthermore, we present the implementation of FEM using an unstructured mesh on an arbitrarily convex domains. In addition, the stability and convergence of the fully discrete scheme is analyzed.

The rest of the paper is organized as follows. In Section 2, we present some notations on irregular domains and the relevant fractional calculus definitions. In Section 3, we derive the fully discrete scheme for the problem (1.2)-(1.4) and describe how the FEM is implemented using unstructured mesh on an arbitrarily convex domain. In Section 4, we establish the stability and convergence of the method. In Section 5, we give some numerical examples to validate theoretical results. Finally, some conclusions are drawn in Section 6.

2. Preliminaries

In this section, we introduce some definitions and lemmas on the fractional derivative spaces established by Ervin and Roop.,[7,8] we denote

$$(u, v) = \int_{a_1}^{b_1} \int_{c(y)}^{r(y)} u(x, y)v(x, y)\mathrm{d}x\mathrm{d}y = \int_{c_1}^{d_1} \int_{g(x)}^{m(x)} u(x, y)v(x, y)\mathrm{d}y\mathrm{d}x,$$

and $\|u\|_{L^2} = (u,u)^{\frac{1}{2}}$.

In the following part, the positive constant C will be used as a generic constant, which is independent of n, τ_n, h and N. It may have different values in different places.

Definition 2.1. (Left Fractional Derivative Space). Let $\mu > 0$, we define the semi-norm and the norm respectively as

$$|u|_{J_L^\mu} = \left(\|_{c(y)} D_x^\mu u\|_{L_2}^2 + \|_{g(x)} D_y^\mu u\|_{L_2}^2 \right)^{\frac{1}{2}}, \quad \|u\|_{J_L^\mu} = \left(\|u\|_{L_2}^2 + |u|_{J_L^\mu}^2 \right)^{\frac{1}{2}},$$

and denote $J_L^\mu(\Omega)(J_{L,0}^\mu(\Omega))$ as the closure of $C^\infty(\Omega)(C_0^\infty(\Omega))$ with respect to $\|\cdot\|_{J_L^\mu}$.

Definition 2.2. (Right Fractional Derivative Space). Let $\mu > 0$, we define the semi-norm and the norm respectively as

$$|u|_{J_R^\mu} = \left(\|_x D_{r(y)}^\mu u\|_{L_2}^2 + \|_y D_{m(x)}^\mu u\|_{L_2}^2 \right)^{\frac{1}{2}}, \quad \|u\|_{J_R^\mu} = \left(\|u\|_{L_2}^2 + |u|_{J_R^\mu}^2 \right)^{\frac{1}{2}},$$

and denote $J_R^\mu(\Omega)(J_{R,0}^\mu(\Omega))$ as the closure of $C^\infty(\Omega)(C_0^\infty(\Omega))$ with respect to $\|\cdot\|_{J_R^\mu}$.

Definition 2.3. (Symmetric Fractional Derivative Space). Let $\mu > 0, \mu \neq n - \frac{1}{2}, n \in N$, we define the semi-norm and the norm respectively as

$$|u|_{J_S^\mu} = \left(|(_{c(y)} D_x^\mu u,\ _x D_{r(y)}^\mu u)| + |(_{g(x)} D_y^\mu u,\ _y D_{m(x)}^\mu u)| \right)^{\frac{1}{2}}, \|u\|_{J_S^\mu} = \left(\|u\|_{L_2}^2 + |u|_{J_S^\mu}^2 \right)^{\frac{1}{2}},$$

and denote $J_S^\mu(\Omega)(J_{S,0}^\mu(\Omega))$ as the closure of $C^\infty(\Omega)(C_0^\infty(\Omega))$ with respect to $\|\cdot\|_{J_S^\mu}$.

Definition 2.4. (Fractional Sobolve Space). Let $\mu > 0$, we define the semi-norm and the norm respectively as

$$|u|_{H^\mu} = \||\xi|^\mu \mathcal{F}(\widehat{u})(\xi)\|_{L_2(\mathbb{R})}, \quad \|u\|_{H^\mu} = \left(\|u\|_{L_2}^2 + |u|_{H^\mu}^2 \right)^{\frac{1}{2}},$$

where $\mathcal{F}(\widehat{u})(\xi)$ is the Fourier transform of $\widehat{u}$, $\widehat{u}$ is the zero extension of u outside Ω, and we denote $H^\mu(\Omega)(H_0^\mu(\Omega))$ as the closure of $C^\infty(\Omega)(C_0^\infty(\Omega))$ with respect to $\|\cdot\|_{H^\mu}$.

Lemma 2.1.[7] *If $\mu > 0$, $\mu \neq n - 1/2, n \in N$, then $J_{L,0}^\mu(\Omega), J_{R,0}^\mu(\Omega), J_{S,0}^\mu(\Omega)$ and $H_0^\mu(\Omega)$ are equivalent with equivalent norms and semi-norms. The following inequality holds:*

$$|u|_{J_{L,0}^\mu(\Omega)},\ |u|_{J_{R,0}^\mu(\Omega)} \leq |u|_{H_0^\mu(\Omega)}.$$

Lemma 2.2.[7] *(Fractional Poincaré-Friedrichs). For any $u \in H_0^\mu(\Omega)$,we have*

$$\|u\|_{L^2(\Omega)} \leq C|u|_{H_0^\mu(\Omega)},$$

where $C = 1/\Gamma(1+\mu)$, and for $0 < s < \mu, s \neq n - 1/2, n \in \mathbf{N}$

$$|u|_{H_0^s(\Omega)} \leq C|u|_{H_0^\mu(\Omega)}.$$

Lemma 2.3.[7] *Let $\mu > 0$, $u \in J^{\mu}_{L,0}(\Omega) \cap J^{\mu}_{R,0}(\Omega)$, then*

$$\begin{aligned}\Big({}_{c(y)}D^{\mu}_{x}u(x,y), {}_{x}D^{\mu}_{r(y)}u(x,y)\Big) &= \cos(\mu\pi)\|{}_{-\infty}D^{\mu}_{x}\widehat{u}(x,y)\|^2_{L^2(\mathbb{R}^2)}\\ &= \cos(\mu\pi)\|{}_{x}D^{\mu}_{+\infty}\widehat{u}(x,y)\|^2_{L^2(\mathbb{R}^2)},\\ \Big({}_{g(x)}D^{\mu}_{y}u(x,y), {}_{y}D^{\mu}_{m(x)}u(x,y)\Big) &= \cos(\mu\pi)\|{}_{-\infty}D^{\mu}_{y}\widehat{u}(x,y)\|^2_{L^2(\mathbb{R}^2)}\\ &= \cos(\mu\pi)\|{}_{y}D^{\mu}_{+\infty}\widehat{u}(x,y)\|^2_{L^2(\mathbb{R}^2)},\end{aligned}$$

where $\widehat{u}$ is the extension of u by zero outside Ω.

3. Fully discrete scheme

In this section, we present the fully discrete scheme for the problem(1.2)-(1.4). The time fractional derivative operator is approximated by the L_1 scheme on a temporal graded mesh and the space fractional derivative is discretized by the finite element method.

3.1. *Temporal graded mesh and truncation error*

Firstly, we discretise Eq. (1.2) in the time direction. Generally, the convergence rates of numerical Caputo derivatives are always limited by the non-smoothness near the initial time. To handle the weak singularity in n at $t = 0$, we use a graded mesh. Let N be a positive integer. Set $t_n = T(\frac{n}{N})^{\delta}$ for $n = 0, 1, \ldots, N$, where the constant mesh grading $\delta \geq 1$ is chosen by the user. If $\delta = 1$, then the mesh is uniform. Set $\tau_n = t_n - t_{n-1}$ for $n = 1, 2, \ldots, N$. We note that

$$\tau_{n+1} = T\Big(\frac{n+1}{N}\Big)^{\delta} - T\Big(\frac{n}{N}\Big)^{\delta} \leq CTN^{-\delta}n^{\delta-1} \quad \text{for } n = 1, 2, \ldots, N-1.$$

For each α_i and $n \geq 1$, we approximate the Caputo fractional derivative ${}^{C}_{0}D^{\alpha_i}_{t}u(x,y,t_n)$ by the well known L_1 formula:

$$\begin{aligned}{}^{C}_{0}D^{\alpha_i}_{t}u(\cdot,t_n) \approx D^{\alpha_i}_{N}u^n &:= \frac{1}{\Gamma(1-\alpha_i)}\sum_{k=0}^{n-1}\frac{u^{k+1}-u^k}{\tau_{k+1}}\int_{t_k}^{t_{k+1}}(t_n-s)^{-\alpha_i}\mathrm{d}s\\ &= \frac{1}{\Gamma(2-\alpha_i)}\sum_{k=0}^{n-1}\frac{u^{k+1}-u^k}{\tau_{k+1}}\Big((t_n-t_k)^{1-\alpha_i}-(t_n-t_{k+1})^{1-\alpha_i}\Big)\\ &= \frac{d^i_{n,1}}{\Gamma(2-\alpha_i)}u^n - \frac{1}{\Gamma(2-\alpha_i)}\sum_{k=1}^{n-1}u^{n-k}(d^i_{n,k}-d^i_{n,k+1}) - \frac{d^i_{n,n}}{\Gamma(2-\alpha_i)}u^0,\end{aligned}$$

where $d^i_{n,k} = \big((t_n - t_{n-k})^{1-\alpha_i} - (t_n - t_{n-k+1})^{1-\alpha_i}\big)/\tau_{n-k+1}$ for $k = 1, 2, \ldots, n$. The mean value theorem shows that

$$d^i_{n,k+1} < d^i_{n,k}, \quad \text{for } 0 \leq k \leq n-1 \leq N-1.$$

Defining the real numbers $\eta_{n,k}^i$ for $i = 1, 2, \ldots, r$, $n = 1, 2, \ldots, N$ and $k = 1, 2, \ldots, N$ by $\eta_{n,k}^i = \frac{l_i d_{n,k}^i}{\Gamma(2-\alpha_i)}$, then

$$\sum_{i=1}^{r} l_i D_N^{\alpha_i} u^n = \sum_{i=1}^{r} \eta_{n,1}^i u^n - \sum_{i=1}^{r}\sum_{k=1}^{n-1} (\eta_{n,k}^i - \eta_{n,k+1}^i) u^{n-k} - \sum_{i=1}^{r} \eta_{n,n}^i u^0. \tag{3.1}$$

The temporal truncation error is bound by the following lemma.

Lemma 3.1.[15] *Let the function $u(x, y, t)$ satisfy $\|\partial_t^p u(\cdot, t)\| \leq C(1 + t^{\alpha_1 - p})$ for $p = 0, 1, 2$ and all $t \in (0, T]$. Then for $i = 1, 2, \ldots, r$ and $n \in 1, 2, \ldots, N$, one has*

$$\| {}_0^C D_t^{\alpha_i} u(\cdot, t_n) - D_N^{\alpha_i} u(\cdot, t_n)\| \leq C n^{-\min\{2-\alpha_1, \delta\alpha_1\}}.$$

3.2. *The fully discrete finite element scheme*

Now, we discretise Eq. (1.2) in the space direction by using the Galerkin finite element method. We divide Ω into some triangular regions. Let $\{T_h\}$ denote some triangulation, $\Omega_h = \{\cup\overline{e_h} | e_h \in T_h\}$ and h represents the maximum diameter of the triangulation. We define the finite element subspace as

$$V_h = \{v_h | v_h \in C(\Omega) \cap H_0^{(1+\beta)/2}(\Omega), v_h|_E \text{ is linear for all } E \in T_h\}.$$

The following analysis is standard,[14] but is given in two dimensions here. For $\theta_1, \theta_2 \in (0, 1)$, we consider the space variable with Dirichlet boundary condition

$$-D_x\Big(k(x, y) D_{\theta_1}^{\beta} u(x, y)\Big) - D_y\Big(k(x, y) D_{\theta_2}^{\beta} u(x, y)\Big) = f(x, y). \tag{3.2}$$

Assume that $k(x, y) \in C^1(\overline{\Omega})$, and $k(x, y)$ is bounded:

$$0 < k_{\min} \leq k(x, y) \leq k_{\max}, \ (x, y) \in \Omega.$$

By using the product rule and dividing by $k(x, y)$, Eq. (3.2) can be transformed into the following equivalent form:

$$-D_x\Big(D_{\theta_1}^{\beta} u\Big) - D_y\Big(D_{\theta_2}^{\beta} u\Big) + K_1 D_{\theta_1}^{\beta} u + K_2 D_{\theta_2}^{\beta} u = g, \tag{3.3}$$

where $K_1 = -\frac{k_x(x,y)}{k(x,y)} \in L^\infty$, $K_2 = -\frac{k_y(x,y)}{k(x,y)} \in L^\infty$, $g = \frac{f(x,y)}{k(x,y)}$. We denote $\gamma = (1+\beta)/2 \in (1/2, 1)$, which represents the order of the equation. Here, we additionally introduce the extra fractional low-order terms $K_1 D_{\theta_1}^{\beta} u$ and $K_2 D_{\theta_2}^{\beta} u$.

Multiplying Eq. (3.3) by $v \in H_0^{\gamma}(\Omega)$ and taking integral by parts, we obtain the variational formulation of Eq. (3.3) as: find $u \in H_0^{\gamma}(\Omega)$, such that

$$A(u, v) = (g, v),$$

where the bilinear form $A(u, v) : H_0^{\gamma}(\Omega) \times H_0^{\gamma}(\Omega) \to \mathbb{R}$ is

$$A(u, v) = \Big(D_{\theta_1}^{\beta} u, D_x v\Big) + \Big(D_{\theta_2}^{\beta} u, D_y v\Big) + \Big(K_1 D_{\theta_1}^{\beta} u, v\Big) + \Big(K_2 D_{\theta_2}^{\beta} u, v\Big).$$

Let u_h be the solution of the finite-dimensional variational problem: find $u_h \in H_0^\gamma(\Omega)$ such that

$$A(u_h, v) = (g, v), \text{ for any } v \in V_h.$$

We apply the nonuniform L_1 scheme (3.1) to discretise Eq. (1.2) in the time direction. The fully discrete scheme for problem (1.2)-(1.4) is: for each $t = t_n (n = 1, 2, \ldots, N)$, find $u_h^n \in V_h$ such that

$$\begin{cases} \Big(\frac{1}{k}\sum_{i=1}^{r} l_i D_N^{\alpha_i} u_h^n, v_h\Big) + A(u_h^n, v_h) = (g^n, v_h), \ \forall v_h \in V_h, \\ u_h^0 = u_{0h}. \end{cases} \tag{3.4}$$

3.3. *The implementation of FEM with an unstructured mesh*

We present the detailed computation process for piecewise linear polynomials on the triangular element $e_p,\ p = 1, 2, \ldots, N_e$, where N_e is the total number of triangles. Similar to,[25] we rewrite u_h^n in the following form:

$$u_h^n = \sum_{i=1}^{N_p} u_i^n l_i(x, y), \tag{3.5}$$

where N_p is the total number of vertices on the convex domain Ω, u_i^n are the coefficients which need to be solved. Substituting Eq. (3.5) into Eq. (3.4) with $v_h = l_j(x, y),\ j = 1, 2, \ldots, N_p$ gives

$$\begin{aligned} &\frac{1}{k}\sum_{s=1}^{r}\eta_{n,1}^s \sum_{i=1}^{N_p} u_i^n (l_i, l_j) + \sum_{i=1}^{N_p} u_i^n A(l_i, l_j) \\ =&\frac{1}{k}\sum_{s=1}^{r}\sum_{i=1}^{N_p}\sum_{k=1}^{n-1}(\eta_{n,k}^s - \eta_{n,k+1}^s) u_i^{n-k}(l_i, l_j) + \frac{1}{k}\sum_{s=1}^{r}\eta_{n,n}^s \sum_{i=1}^{N_p} u_i^0 (l_i, l_j) + (g^n, l_j). \end{aligned} \tag{3.6}$$

Eq. (3.6) can be expressed in the matrix form

$$\sum_{s=1}^{r}\eta_{n,1}^s MU^n + BU^n = \sum_{s=1}^{r}\sum_{k=1}^{n-1}(\eta_{n,k}^s - \eta_{n,k+1}^s) MU^{n-k} + \sum_{s=1}^{r}\eta_{n,n}^s MU^0 + F^n, \tag{3.7}$$

where M is the mass matrix with elements $M_{ij} = (l_j, l_i)$, B is the stiffness matrix with elements $B_{ij} = k \cdot A(l_j, l_i)$, $U^n = [u_1^n, u_2^n, \ldots, u_{N_p}^n]^T$ and $F^n = [(f^n, l_1), (f^n, l_2), \ldots, (f^n, l_{N_p})]^T$. Due to the non-local property of the fractional operator, the matrix B is the most difficult part to calculate. The (i, j) entry of the

matrix B is given by

$$\begin{aligned} B_{ij} = k \cdot A(l_j, l_i) = & - k\theta_1 \Big({}_{c(y)}D_x^{\gamma}\ l_j, {}_xD_{r(y)}^{\gamma}\ l_i \Big) - k(1-\theta_1) \Big({}_xD_{r(y)}^{\gamma}\ l_j, {}_{c(y)}D_x^{\gamma}\ l_i \Big) \\ & - k\theta_2 \Big({}_{g(x)}D_y^{\gamma}\ l_j, {}_yD_{m(x)}^{\gamma}\ l_i \Big) - k(1-\theta_2) \Big({}_yD_{m(x)}^{\gamma}\ l_j, {}_{g(x)}D_y^{\gamma}\ l_i \Big) \\ & - k_x\theta_1 \Big({}_{c(y)}D_x^{\beta}\ l_j,\ l_i \Big) + k_x(1-\theta_1) \Big({}_xD_{r(y)}^{\beta} l_j,\ l_i \Big) \\ & - k_y\theta_2 \Big({}_{g(x)}D_y^{\beta}\ l_j,\ l_i \Big) + k_y(1-\theta_2) \Big({}_yD_{m(x)}^{\beta}\ l_j,\ l_i \Big). \end{aligned} \tag{3.8}$$

Noticing the similarity of the right hand side of Eq. (3.8), we will illustrate the computation of $k\Big({}_{c(y)}D_x^{\gamma}\ l_j, {}_xD_{r(y)}^{\gamma}\ l_i \Big)$ and $k_x\Big({}_{c(y)}D_x^{\beta}\ l_j,\ l_i \Big)$ as examples. By applying Gauss quadrature, we obtain

$$\begin{aligned} & k\Big({}_{c(y)}D_x^{\gamma}\ l_j, {}_xD_{r(y)}^{\gamma}\ l_i \Big) = k \sum_{p=1}^{N_e} \int_{e_p} {}_{c(y)}D_x^{\gamma}\ l_j\ {}_xD_{r(y)}^{\gamma}\ l_i \mathrm{dxdy} \\ \approx & \sum_{p=1}^{N_e} \sum_{(\widehat{x}_q, \widehat{y}_q) \in G_K} \omega_q\ {}_{c(y)}D_x^{\gamma} l_j|_{(\widehat{x}_q, \widehat{y}_q)} \cdot {}_xD_{r(y)}^{\gamma} l_i|_{(\widehat{x}_q, \widehat{y}_q)} \cdot k(\widehat{x}_q, \widehat{y}_q), \\ & k_x\Big({}_{c(y)}D_x^{\beta}\ l_j,\ l_i \Big) = k_x \sum_{p=1}^{N_e} \int_{e_p} {}_{c(y)}D_x^{\beta} l_j l_i \mathrm{dxdy} \\ \approx & \sum_{p=1}^{N_e} \sum_{(\widehat{x}_q, \widehat{y}_q) \in G_K} \omega_q\ {}_{c(y)}D_x^{\beta} l_j|_{(\widehat{x}_q, \widehat{y}_q)} \cdot l_i|_{(\widehat{x}_q, \widehat{y}_q)} \cdot k_x(\widehat{x}_q, \widehat{y}_q), \end{aligned}$$

where G_k is the set of all Gauss points in element e_p and ω_q are the weights associated with the Gauss point $p(\widehat{x}_q, \widehat{y}_q)$. Finally, we present the whole computation process in the following algorithm (see Algorithm 3.3). For details on how to calculation the fractional derivatives of the basis function $l_i(x, y)$, please see.[25]

4. Stability and convergence of the fully discrete scheme

In this section, we consider the stability and convergence of the fully discrete scheme (3.4). First, we prove the continuity and coercivity of the bilinear form $A(u, v)$. For the convenience of proof, we divide it into the following two parts:

$$A(u, v) = A_1(u, v) + A_2(u, v),$$

Algorithm 3.3. Compiling fractional derivative using FEM on an unstructured mesh

1: Partition the convex domain Ω with unstructured triangular elements e_p and save the element information (node number, coordinates, and element number);
2: **for** each element $p = 1, 2, \ldots, N_e$ **do**
3: Find the Gauss point $(\widehat{x}_q, \widehat{y}_q)$ and weights ω_i on each triangles element e_p;
4: **for** each Gauss point $j = 1, 2, \ldots, N_p$ **do**
5: Find the points of intersection by $y = \widehat{y}_q$ with Ω_{e_j}, compute ${}_{c(y)}D_x^{\gamma} l_j|_{(\widehat{x}_q,\widehat{y}_q)}$, ${}_{x}D_{r(y)}^{\gamma} l_i|_{(\widehat{x}_q,\widehat{y}_q)}$ and ${}_{c(y)}D_x^{\beta} l_j|_{(\widehat{x}_q,\widehat{y}_q)}$, $l_i|_{(\widehat{x}_q,\widehat{y}_q)}$;
6: Find the points of intersection by $x = \widehat{x}_q$ with Ω_{e_j}, compute ${}_{g(x)}D_y^{\gamma} l_j|_{(\widehat{x}_q,\widehat{y}_q)}$, ${}_{y}D_{m(x)}^{\gamma} l_i|_{(\widehat{x}_q,\widehat{y}_q)}$ and ${}_{g(x)}D_y^{\beta} l_j|_{(\widehat{x}_q,\widehat{y}_q)}$, $l_i|_{(\widehat{x}_q,\widehat{y}_q)}$;
7: **end for**
8: Form stiffness matrix A;
9: **end for**
10: Calculate $(l_j, l_i)_{e_p}$ on each triangle element e_p to form the mass matrix M;
11: Calculate $(f^n, l_k)_{e_p}$, $k = 1, 2, \ldots, N_p$ and obtain F^n;
12: Solve the linear system (3.7) , then obtain U^n.

where

$$\begin{aligned}
A_1(u,v) =& \Big(D_{\theta_1}^{\beta} u, D_x v\Big) + \Big(D_{\theta_2}^{\beta} u, D_y v\Big) \\
=& -\theta_1 \Big({}_{c(y)}D_x^{\gamma} u, {}_{x}D_{r(y)}^{\gamma} v\Big) - (1-\theta_1)\Big({}_{x}D_{r(y)}^{\gamma} u, {}_{c(y)}D_x^{\gamma} v\Big) \\
& -\theta_2 \Big({}_{g(x)}D_y^{\gamma} u, {}_{y}D_{m(x)}^{\gamma} v\Big) - (1-\theta_2)\Big({}_{y}D_{m(x)}^{\gamma} u, {}_{g(x)}D_y^{\gamma} v\Big), \\
A_2(u,v) =& \Big(K_1 D_{\theta_1}^{\beta} u, v\Big) + \Big(K_2 D_{\theta_2}^{\beta} u, v\Big) \\
=& \theta_1 \Big(K_1 \, {}_{c(y)}D_x^{\beta} u, v\Big) - (1-\theta_1)\Big(K_1 \, {}_{x}D_{r(y)}^{\beta} u, v\Big) \\
& + \theta_2 \Big(K_2 \, {}_{g(x)}D_y^{\beta} u, v\Big) - (1-\theta_2)\Big(K_2 \, {}_{y}D_{m(x)}^{\beta} u, v\Big).
\end{aligned}$$

Lemma 4.1. *Let* $\widetilde{\theta} = \max\{\theta_1, \theta_2, (1-\theta_1), (1-\theta_2)\}$ *and* $K_1, K_2 \in L^{\infty}(\Omega)$, $K = \max\{|K_1|, |K_2|\}$. *Then for any* $u, v \in H_0^{\gamma}(\Omega)$ *and* Ω *being a convex domain, there exists a constant* C *such that*

$$A(u,v) \le C \|u\|_{H_0^{\gamma}(\Omega)} \|v\|_{H_0^{\gamma}(\Omega)}.$$

Proof. According to the definition of $A_1(u,v)$ and the Cauchy-Schwarz inequality, we have

$$\begin{aligned}
A_1(u,v) \le& \theta_1 \|{}_{c(y)}D_x^{\gamma} u\| \|{}_{x}D_{r(y)}^{\gamma} v\| + \theta_2 \|{}_{g(x)}D_y^{\gamma} u\| \|{}_{y}D_{m(x)}^{\gamma} v\| \\
& + (1-\theta_1) \|{}_{x}D_{r(y)}^{\gamma} u\| \|{}_{c(y)}D_x^{\gamma} v\| + (1-\theta_2) \|{}_{y}D_{m(x)}^{\gamma} u\| \|{}_{g(x)}D_y^{\gamma} v\|.
\end{aligned}$$

By using the inequality $a_1b_1 + a_2b_2 \leq \sqrt{a_1^2 + a_2^2}\sqrt{b_1^2 + b_2^2}$, $a_1, a_2, b_1, b_2 > 0$, we obtain

$$\begin{aligned}A_1(u,v) \leq & \sqrt{\theta_1\|_{c(y)}D_x^\gamma u\|^2 + \theta_2\|_{g(x)}D_y^\gamma u\|^2}\sqrt{\theta_1\|_x D^\gamma_{r(y)}v\|^2 + \theta_2\|_y D^\gamma_{m(x)}v\|^2} \\ & + \sqrt{(1-\theta_1)\|_x D^\gamma_{r(y)}u\|^2 + (1-\theta_2)\|_y D^\gamma_{m(x)}u\|^2} \\ & \sqrt{(1-\theta_1)\|_{c(y)}D_x^\gamma v\|^2 + (1-\theta_2)\|_{g(x)}D_y^\gamma v\|^2} \\ \leq & \widetilde{\theta}\Big(|u|_{J^\gamma_{L,0}(\Omega)}|v|_{J^\gamma_{R,0}(\Omega)} + |u|_{J^\gamma_{R,0}(\Omega)}|v|_{J^\gamma_{L,0}(\Omega)}\Big).\end{aligned}$$

Combining with Lemma 2.1, we have

$$A_1(u,v) \leq 2\widetilde{\theta}|u|_{H_0^\gamma(\Omega)}|v|_{H_0^\gamma(\Omega)} \leq 2\widetilde{\theta}\|u\|_{H_0^\gamma(\Omega)}\|v\|_{H_0^\gamma(\Omega)}.$$

According to the definition of $A_2(u,v)$ and the Cauchy-Schwarz inequality, we obtain

$$\begin{aligned}A_2(u,v) \leq & \theta_1\|K_1\|_{L^\infty}\|_{c(y)}D_x^\beta u\|\|v\| + (1-\theta_1)\|K_1\|_{L^\infty}\|_x D^\beta_{r(y)}u\|\|v\| \\ & + \theta_2\|K_2\|_{L^\infty}\|_{g(x)}D_y^\beta u\|\|v\| + (1-\theta_2)\|K_2\|_{L^\infty}\|_y D^\beta_{m(x)}u\|\|v\| \\ \leq & \widetilde{\theta}\|K\|_{L^\infty}\|v\|\Big(\|_{c(y)}D_x^\beta u\| + \|_{g(x)}D_y^\beta u\| + \|_x D^\beta_{r(y)}u\| + \|_y D^\beta_{m(x)}u\|\Big).\end{aligned}$$

Utilising the inequality $a_1 + a_2 \leq \sqrt{2(a_1^2 + a_2^2)}$, $a_1, a_2 > 0$, we have

$$\begin{aligned}A_2(u,v) \leq & \widetilde{\theta}\|K\|_{L^\infty}\|v\|\Bigg(\sqrt{2\Big(\|_{c(y)}D_x^\beta u\|^2 + \|_{g(x)}D_y^\beta u\|^2\Big)} \\ & + \sqrt{2\Big(\|_x D^\beta_{r(y)}v\|^2 + \|_y D^\beta_{m(x)}v\|^2\Big)}\Bigg) \\ \leq & \sqrt{2}\widetilde{\theta}\|K\|_{L^\infty}\|v\|\Big(|u|_{J^\beta_{L,0}(\Omega)} + |u|_{J^\beta_{R,0}(\Omega)}\Big).\end{aligned}$$

According to Lemma 2.1 and Lemma 2.2 we get

$$A_2(u,v) \leq 2\sqrt{2}\widetilde{\theta}\|K\|_{L^\infty}\|v\||u|_{H_0^\beta(\Omega)} \leq C\|K\|_{L^\infty}\|u\|_{H_0^\gamma(\Omega)}\|v\|_{H_0^\gamma(\Omega)}.$$

Thus, $A(u,v) \leq C\|u\|_{H_0^\gamma(\Omega)}\|v\|_{H_0^\gamma(\Omega)}$. □

Lemma 4.2. *Let* $\widetilde{\theta} = \max\{\theta_1, \theta_2, (1-\theta_1), (1-\theta_2)\}$ *and* $K_1, K_2 \in L^\infty(\Omega)$, $K = \max\{|K_1|, |K_2|\}$ *satisfy*

$$\|K\|_\infty < \frac{\cos(\beta\pi/2)}{\sqrt{2}\widetilde{\theta}\Big(1 + \big(1/\Gamma((3+\beta)/2)\big)^2\Big)}. \tag{4.1}$$

Then there exists a positive constant $C(\beta, K, \widetilde{\theta})$ *such that for any* $u \in H_0^\gamma(\Omega)$,

$$A(u,u) \geq C(\beta, K, \widetilde{\theta})\|u\|^2_{H_0^\gamma(\Omega)}.$$

Proof. According to the definition of $A_1(u,u)$ and Lemma 2.3, we have

$$\begin{aligned}A_1(u,u) &= -\Big({}_{c(y)}D_x^{\gamma}u, {}_xD_{r(y)}^{\gamma}u\Big) - \Big({}_{g(x)}D_y^{\gamma}u, {}_yD_{m(x)}^{\gamma}u\Big)\\ &\geq -\cos(\gamma\pi)\Big(\|{}_{c(y)}D_x^{\gamma}u\|^2 + \|{}_{g(x)}D_y^{\gamma}u\|^2\Big) = -\cos(\gamma\pi)|u|^2_{J^{\gamma}_{L,0}(\Omega)}.\end{aligned}$$

Using Lemma 2.1, we obtain

$$A_1(u,u) \geq -\cos(\gamma\pi)|u|^2_{H_0^{\gamma}(\Omega)} = \cos(\beta\pi/2)|u|^2_{H_0^{\gamma}(\Omega)}.$$

By the fractional Poincaré-Friedrichs inequality, Lemma 2.2,

$$\|u\|_{L^2(\Omega)} \leq \frac{1}{\Gamma(1+\gamma)}|u|_{H_0^{\gamma}(\Omega)}.$$

It then holds that

$$\|u\|^2_{H_0^{\gamma}(\Omega)} = \|u\|^2_{L^2(\Omega)} + |u|^2_{H_0^{\gamma}(\Omega)} \leq \left(1 + \Big(\frac{1}{\Gamma(1+\gamma)}\Big)^2\right)|u|^2_{H_0^{\gamma}(\Omega)}.$$

Therefore,

$$A_1(u,u) \geq \cos(\beta\pi/2)|u|^2_{H_0^{\gamma}(\Omega)} \geq \frac{\cos(\beta\pi/2)}{1+\big(1/\Gamma(1+\gamma)\big)^2}\|u\|^2_{H_0^{\gamma}(\Omega)}.$$

According to the definition of $A_2(u,u)$ and the Cauchy-Schwarz inequality, we obtain

$$\begin{aligned}A_2(u,u) \geq& -\theta_1\|K_1\|_{L^{\infty}}\|{}_{c(y)}D_x^{\beta}u\|\|u\| - (1-\theta_1)\|K_1\|_{L^{\infty}}\|{}_xD_{r(y)}^{\beta}u\|\|u\|\\ &-\theta_2\|K_2\|_{L^{\infty}}\|{}_{g(x)}D_y^{\beta}u\|\|u\| - (1-\theta_2)\|K_2\|_{L^{\infty}}\|{}_yD_{m(x)}^{\beta}u\|\|u\|\\ \geq& -\widetilde{\theta}\|K\|_{L^{\infty}}\|u\|\Big(\|{}_{c(y)}D_x^{\beta}u\| + \|{}_{g(x)}D_y^{\beta}u\| + \|{}_xD_{r(y)}^{\beta}u\| + \|{}_yD_{m(x)}^{\beta}u\|\Big),\end{aligned}$$

Utilising the inequality $a_1 + a_2 \leq \sqrt{2(a_1^2+a_2^2)}, \quad a_1, a_2 > 0$, we have

$$A_2(u,u) \geq -\sqrt{2}\widetilde{\theta}\|K\|_{L^{\infty}}\|u\|\Big(|u|_{J^{\beta}_{L,0}(\Omega)} + |u|_{J^{\beta}_{R,0}(\Omega)}\Big).$$

Using Lemma 2.1 and inequality $a^2 + b^2 \geq 2ab, \quad a,\ b > 0$, yields

$$\begin{aligned}A_2(u,u) &\geq -2\sqrt{2}\widetilde{\theta}\|K\|_{L^{\infty}}\|u\||u|_{H_0^{\beta}(\Omega)} \geq -\sqrt{2}\widetilde{\theta}\|K\|_{L^{\infty}}(\|u\|^2_{L^2(\Omega)} + |u|^2_{H_0^{\beta}(\Omega)})\\ &= -\sqrt{2}\widetilde{\theta}\|K\|_{L^{\infty}}\|u\|^2_{H_0^{\beta}(\Omega)} \geq -\sqrt{2}\widetilde{\theta}\|K\|_{L^{\infty}}\|u\|^2_{H_0^{\gamma}(\Omega)}.\end{aligned}$$

Therefore the bilinear form is bounded below as

$$A(u,u) \geq \left(\frac{\cos(\beta\pi/2)}{1+\big(1/\Gamma(1+\gamma)\big)^2} - \sqrt{2}\widetilde{\theta}\|K\|_{L^{\infty}}\right)\|u\|^2_{H_0^{\gamma}(\Omega)}.$$

(4.1) implies that

$$C(\beta, K, \widetilde{\theta}) = \frac{\cos(\beta\pi/2)}{1+\big(1/\Gamma(1+\gamma)\big)^2} - \sqrt{2}\widetilde{\theta}\|K\|_{L^{\infty}} > 0.$$

□

We also need the following two lemmas for the theoretical analysis.

Lemma 4.3.[15] *Let the functions $v^j = v(\cdot, t^j)$ be in $L^2(\Omega)$ for $j = 0, 1, \ldots, N$. Then the discrete $L1$ scheme satisfies*

$$\Big(\sum_{i=1}^{r} l_i D_N^{\alpha_i} v^n, v^n\Big) \geq \Big(\sum_{i=1}^{r} l_i D_N^{\alpha_i} \|v^n\|\Big)\|v^n\| \quad \text{for } n = 1, 2, \ldots, N.$$

Lemma 4.4.[15] *Assume that the sequences $\{\xi^n\}_{n=1}^N$ and $\{\sigma^n\}_{n=1}^N$ are non-negative, that $V^0 \geq 0$, and that the sequence $\{V^n\}_{n=1}^N$ satisfies*

$$V^n \sum_{i=1}^{r} l_i D_N^{\alpha_i} V^n \leq \xi^n V^n + (\sigma^n)^2 \quad \text{for } n = 1, 2, \ldots, N.$$

Then

$$V^n \leq V^0 + \Gamma(1-\alpha_1) \max_{j=1,\ldots,n} \{t_j^{\alpha_1} \xi^j\} + \sqrt{\Gamma(1-\alpha_1)} \max_{j=1,\ldots,n} \{t_j^{\alpha_1/2} \sigma^j\} \quad \text{for } n = 1, 2, \ldots, N.$$

Theorem 4.1. *(Stability) The fully discrete scheme* (3.4) *is unconditionally stable, and it holds that*

$$\|u_h^n\| \leq \|u_h^0\| + T^{\alpha_1} \Gamma(1-\alpha_1) \widetilde{k} \max_{j=1,2,\ldots,n} \|f^j\| \quad \text{for } n = 1, 2, \ldots, N.$$

where $\widetilde{k} = k_{\max}/k_{\min}$.

Proof. In the fully discrete scheme (3.4), letting $v = u_h^n$, we have

$$\Big(\frac{1}{k} \sum_{i=1}^{r} l_i D_N^{\alpha_i} u_h^n, u_h^n\Big) + A(u_h^n, u_h^n) = (g^n, u_h^n).$$

According to Lemma 4.2, discarding the non-negative term $A(u_h^n, u_h^n)$, we obtain

$$\Big(\frac{1}{k} \sum_{i=1}^{r} l_i D_N^{\alpha_i} u_h^n, u_h^n\Big) \leq (g^n, u_h^n). \tag{4.2}$$

Letting $\overline{u}_h^n = \frac{u_h^n}{\sqrt{k}}$, by Lemma 4.3, the left-hand-side of (4.2) can be estimated as

$$\begin{aligned}\Big(\frac{1}{k} \sum_{i=1}^{r} l_i D_N^{\alpha_i} u_h^n, u_h^n\Big) &= \Big(\sum_{i=1}^{r} l_i D_N^{\alpha_i} \overline{u}_h^n, \overline{u}_h^n\Big) \geq \Big(\sum_{i=1}^{r} l_i D_N^{\alpha_i} \|\overline{u}_h^n\|\Big)\|\overline{u}_h^n\| \\ &\geq \Big(\frac{1}{k_{\max}} \sum_{i=1}^{r} l_i D_N^{\alpha_i} \|u_h^n\|\Big)\|u_h^n\|. \end{aligned} \tag{4.3}$$

By using the Cauchy-Schwarz inequality, we obtain the following estimate for the right-hand-side of (4.2):

$$(g^n, u_h^n) = \Big(\frac{f^n}{k}, u_h^n\Big) \leq \Big\|\frac{f^n}{k}\Big\| \|u_h^n\| \leq \frac{1}{k_{\min}} \|f^n\| \|u_h^n\|. \tag{4.4}$$

Substituting (4.3) and (4.4) into (4.2) yields

$$\Big(\frac{1}{k_{\max}} \sum_{i=1}^{r} l_i D_N^{\alpha_i} \|u_h^n\|\Big)\|u_h^n\| \leq \frac{1}{k_{\min}} \|f^n\| \|u_h^n\|.$$

Using Lemma 4.4, we obtain

$$\begin{aligned}\|u_h^n\| \leq & \|u_h^0\| + \Gamma(1-\alpha_1)\widetilde{k} \max_{j=1,2,\ldots,n}\{t_j^{\alpha_1}\|f^j\|\} \\ \leq & \|u_h^0\| + T^{\alpha_1}\Gamma(1-\alpha_1)\widetilde{k} \max_{j=1,2,\ldots,n}\|f^j\|.\end{aligned}$$

The proof is completed. □

We define the projection operator P_h as the orthogonal projection with respect to the inner product $A(u,v)$ such that

$$A(P_h u, v) = A(u,v), \forall v \in V_h, \text{ for } u \in H_0^\gamma(\Omega).$$

We assume there is an interpolation operator I_h from H^2 to V_h such that

$$\|u - I_h u\|_{H^s(\Omega)} \leq Ch^{\mu-s}\|u\|_{H^\mu(\Omega)}, \forall u \in H^\mu(\Omega),\ 0 \leq s < \mu \leq 2.$$

Lemma 4.5.[7] *Assuming that the solution u of the variational form $A(u,v) = (f,v)$ satisfies*

$$\|u\|_{H^{2\gamma}(\Omega)} \leq C\|f\|_{L^2(\Omega)},$$

then we have

$$\begin{aligned}&\|u - P_h u\|_{L^2(\Omega)} \leq Ch^2\|u\|_{H^2(\Omega)},\ \gamma \neq 3/4. \\ &\|u - P_h u\|_{L^2(\Omega)} \leq Ch^{2-\epsilon}\|u\|_{H^{2-\epsilon}(\Omega)},\ \gamma = 3/4,\ 0 < \epsilon < 1.\end{aligned}$$

Theorem 4.2. *(Convergence) Let $K \in L^\infty(\Omega)$ satisfy (4.1) and $\|\partial_t^p u(\cdot,t)\| \leq C(1+t^{\alpha_1-p})$ for $p = 0,1,2$ and all $t \in (0,T]$. Suppose $u_h^n, u(t_n)$ are numerical solution and exact solution of problem (1.2)-(1.4) at $t = t_n$ respectively, and $u, u_t, {}_0D_t^{\alpha_i} u \in L^2(0,T;H^2(\Omega))$. When we choose the triangular linear basis function, the error satisfies*

$$\|u^n - u_h^n\| \leq C(h^{2-\epsilon} + N^{-\min\{2-\alpha_1, \delta\alpha_1\}}).$$

Here, $\epsilon = 0$ when $\gamma \neq 3/4$ while $0 < \epsilon < 1/2$ when $\gamma = 3/4$.

Proof. According to Eq. (1.2) and fully discrete scheme (3.4), letting $e^n = u(t_n) - u_h^n$, we obtain

$$\Big(\frac{1}{k}\sum_{i=1}^r l_i D_N^{\alpha_i} e^n, v_h\Big) + A(e^n, v_h) = -(\phi^n, v_h),$$

where $\phi^n(x) := \frac{1}{k}\sum\limits_{i=1}^r l_i\big({}_0^C D_t^{\alpha_i} u(x,y,t_n) - D_N^{\alpha_i} u(x,y,t_n)\big)$. Defining $\rho^n = P_h u(t_n) - u(t_n)$, $\theta^n = P_h u(t_n) - u_h^n$, taking $v_h = \theta^n$ in above equation, then we have

$$\Big(\frac{1}{k}\sum_{i=1}^r l_i D_N^{\alpha_i}\theta^n, \theta^n\Big) + A(\theta^n, \theta^n) = \Big(\frac{1}{k}\sum_{i=1}^r l_i D_N^{\alpha_i}\rho^n, \theta^n\Big) - (\phi^n, \theta^n). \tag{4.5}$$

Clearly

$$D_N^{\alpha_i}\rho^n = D_N^{\alpha_i}\rho^n - {}_0^C D_t^{\alpha_i}\rho^n + {}_0^C D_t^{\alpha_i}\rho^n$$
$$= \Big({}_0^C D_t^{\alpha_i} u(x,t_n) - D_N^{\alpha_i} u(x,t_n)\Big) - P_h\Big({}_0^C D_t^{\alpha_i} u(x,t_n) - D_N^{\alpha_i} u(x,t_n)\Big) + {}_0^C D_t^{\alpha_i}\rho^n. \tag{4.6}$$

Substituting (4.6) into (4.5) yields

$$\Big(\frac{1}{k}\sum_{i=1}^{r} l_i D_N^{\alpha_i}\theta^n, \theta^n\Big) + A(\theta^n,\theta^n) = \Big(\frac{1}{k}\sum_{i=1}^{r} l_i\, {}_0^C D_t^{\alpha_i}\rho^n, \theta^n\Big) - (P_h\phi^n, \theta^n). \tag{4.7}$$

Recalling Lemma 4.2 and Lemma 4.3, we can obtain the following estimate for the left-hand-side of (4.7):

$$\Big(\frac{1}{k}\sum_{i=1}^{r} l_i D_N^{\alpha_i}\theta^n, \theta^n\Big) + A(\theta^n,\theta^n) \geq \Big(\frac{1}{k_{\max}}\sum_{i=1}^{r} l_i D_N^{\alpha_i}\|\theta^n\|\Big)\|\theta^n\| + C_1\|\theta^n\|_{H^\gamma}^2. \tag{4.8}$$

According to the Cauchy-Schwarz inequality and the inequality $ab \leq \varepsilon a^2 + \frac{b^2}{4\varepsilon}$ ($\varepsilon > 0$), the first term on the right-hand-side of (4.7) can be estimated as

$$\Big(\frac{1}{k}\sum_{i=1}^{r} l_i\, {}_0^C D_t^{\alpha_i}\rho^n, \theta^n\Big) \leq \|\frac{1}{k}\sum_{i=1}^{r} l_i\, {}_0^C D_t^{\alpha_i}\rho^n\|\|\theta^n\| \leq \frac{1}{4\varepsilon}\|\frac{1}{k}\sum_{i=1}^{r} l_i\, {}_0^C D_t^{\alpha_i}\rho^n\|^2 + \varepsilon\|\theta^n\|^2$$
$$\leq \frac{1}{4\varepsilon}\|\frac{1}{k}\sum_{i=1}^{r} l_i\, {}_0^C D_t^{\alpha_i}\rho^n\|^2 + \varepsilon C_2\|\theta^n\|_{H^\gamma}^2. \tag{4.9}$$

By the Cauchy-Schwarz inequality and Lemma 4.5, the second term on the right-hand-side of (4.7) can be estimated as

$$(P_h\phi^n, \theta^n) \leq \|P_h\phi^n\|\|\theta^n\| \leq \Big(\|P_h\phi^n - \phi^n\| + \|\phi^n\|\Big)\|\theta^n\|$$
$$\leq \Big(Ch^{2-\epsilon}\|\phi^n\|_{H^{2-\epsilon}} + \|\phi^n\|\Big)\|\theta^n\| \leq C\|\phi^n\|\|\theta^n\|, \tag{4.10}$$

Substituting (4.8), (4.9) and (4.10) into (4.7), and letting $\varepsilon = \frac{C_1}{C_2}$ gives

$$\Big(\frac{1}{k_{\max}}\sum_{i=1}^{r} l_i D_N^{\alpha_i}\|\theta^n\|\Big)\|\theta^n\| \leq \frac{C_2}{4C_1}\|\frac{1}{k}\sum_{i=1}^{r} l_i\, {}_0^C D_t^{\alpha_i}\rho^n\|^2 + C\|\phi^n\|\|\theta^n\|.$$

Using Lemma 4.5 again and the assumed condition ${}_0^C D_t^{\alpha_i} u \in L^2(0,T;H^2(\Omega))$, we obtain

$$\Big(\sum_{i=1}^{r} l_i D_N^{\alpha_i}\|\theta^n\|\Big)\|\theta^n\| \leq Ch^{2-\epsilon}\sum_{i=1}^{r}\|\, {}_0^C D_t^{\alpha_i} u\|_{H^{2-\epsilon}}^2 + C\|\phi^n\|\|\theta^n\|$$
$$\leq Ch^{2-\epsilon} + C\|\phi^n\|\|\theta^n\|.$$

By Lemma 4.4 and $\|\theta^0\| = \|P_h u^0 - u^0\| = 0$, we get

$$\|\theta^n\| \leq \|\theta^0\| + C\Gamma(1-\alpha_1)\max_{j=1,2,\ldots,n}\{t_j^{\alpha_1}\|\phi^j\|\} + Ch^{2-\epsilon}\sqrt{T^{\alpha_1}\Gamma(1-\alpha_1)}$$
$$= C\Gamma(1-\alpha_1)\max_{j=1,2,\ldots,n}\{t_j^{\alpha_1}\|\phi^j\|\} + Ch^{2-\epsilon}\sqrt{T^{\alpha_1}\Gamma(1-\alpha_1)}. \tag{4.11}$$

By Lemma 3.1, we have $\|\phi^j\| \le Cj^{-\min\{2-\alpha_1,\delta\alpha_1\}}$ and

$$t_j^{\alpha_1} = T^{\alpha_1}\Big(\frac{j}{N}\Big)^{\delta\alpha_1} \le T^{\alpha_1}\Big(\frac{j}{N}\Big)^{\min\{2-\alpha_1,\delta\alpha_1\}}.$$

Since $j/N \le 1$, substituting this inequality into (4.11) yields

$$\|\theta^n\| \le C\Gamma(1-\alpha_1)T^{\alpha_1}N^{-\min\{2-\alpha_1,\delta\alpha_1\}} + Ch^{2-\epsilon}\sqrt{T^{\alpha_1}\Gamma(1-\alpha_1)}.$$

Then we have

$$\|P_h u^n - u_h^n\| \le C(h^{2-\epsilon} + N^{-\min\{2-\alpha_1,\delta\alpha_1\}}).$$

It follows that

$$\|u^n - u_h^n\| \le C(h^{2-\epsilon} + N^{-\min\{2-\alpha_1,\delta\alpha_1\}}).$$

This completes the proof of the theorem. □

5. Numerical examples

In this section, we present three numerical examples to verify the effectiveness of our theoretical analysis.

Example 5.1. Firstly, we consider the following time and space fractional diffusion equation defined on a rectangular domain

$$\begin{cases} l_1\,{}_0^C D_t^{\alpha_1}u(x,y,t) + l_2\,{}_0^C D_t^{\alpha_2}u(x,y,t) + l_3\,{}_0^C D_t^{\alpha_3}u(x,y,t) - D_x\Big(k(x,y)D_{\theta_1}^{\beta}u(x,y,t)\Big) \\ -D_y\Big(k(x,y)D_{\theta_2}^{\beta}u(x,y,t)\Big) = f(x,y,t), \quad (x,y,t)\in\Omega\times(0,T], \\ u(x,y,0) = 0, \ (x,y)\in\overline{\Omega}, \\ u(x,y,t) = 0, \ (x,y,t)\in\partial\Omega\times(0,T], \end{cases}$$

where $\Omega = (0,1)\times(0,1)$, $T = 1$,

$$\begin{aligned} f(x,y,t) &= \Big(\frac{l_1\Gamma(4)t^{3-\alpha_1}}{\Gamma(4-\alpha_1)} + \frac{l_2\Gamma(4)t^{3-\alpha_2}}{\Gamma(4-\alpha_2)} + \frac{l_3\Gamma(4)t^{3-\alpha_3}}{\Gamma(4-\alpha_3)} + l_1\Gamma(1+\alpha_1) \\ &+ \frac{l_2\Gamma(1+\alpha_1)t^{\alpha_1-\alpha_2}}{\Gamma(1+\alpha_1-\alpha_2)} + \frac{l_3\Gamma(1+\alpha_1)t^{\alpha_1-\alpha_3}}{\Gamma(1+\alpha_1-\alpha_3)}\Big)x^2(1-x)^2y^2(1-y)^2 \\ &- (1+t^2)y^2(1-y)^2\Big[k_x(x,y)\big(\theta_1 p(x,\beta) - (1-\theta_1)p(1-x,\beta)\big) \\ &+ k(x,y)\big(\theta_1 p(x,1+\beta) + (1-\theta_1)p(1-x,1+\beta)\big)\Big] \\ &- (1+t^2)x^2(1-x)^2\Big[k_y(x,y)\big(\theta_2 p(y,\beta) - (1-\theta_2)p(1-y,\beta)\big) \\ &+ k(x,y)\big(\theta_2 p(y,1+\beta) + (1-\theta_2)p(1-y,1+\beta)\big)\Big], \\ p(z,\beta) &= \frac{\Gamma(3)}{\Gamma(3-\beta)}z^{2-\beta} - \frac{2\Gamma(4)}{\Gamma(4-\beta)}z^{3-\beta} + \frac{\Gamma(5)}{\Gamma(5-\beta)}z^{4-\beta}. \end{aligned}$$

The exact solution is $u(x,y,t) = (t^{\alpha_1}+t^3)x^2(1-x)^2y^2(1-y)^2$.

We run the simulation by choosing $\alpha_1 = 0.6$, $\alpha_2 = 0.5$, $\alpha_2 = 0.4$, $l_1 = 1, l_2 = 1, l_3 = 1$, $\theta_1 = 0.4$, $\theta_2 = 0.6$, $k(x, y) = e^{0.01x-0.01y}$. Fig.2 shows the rectangular domain partitioned by unstructured triangular meshes for different h. The convergence orders both in time and in space are given in Table 1 and Table 2. For the space direction, the convergence orders in the L^2 norm are shown in Table 1. As is shown in the table, with different choices of the fractional orders, the order in the L^2 norm is about 2, which agrees with the theoretical analysis. For the time direction, based on the theoretical results, the convergence order should be $N^{-\min\{2-\alpha_1,\delta\alpha_1\}}$. As is shown in Table 2, with different fractional orders, the numerical results coincide with Theorem 4.2, indicating the validity of the proposed method.

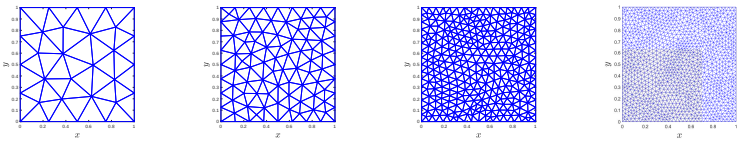

Fig. 2. The rectangular domain partitioned by unstructured meshes used in the calculation for $h \approx 3.1123 \times 10^{-1}$, 1.6759×10^{-1}, 8.6682×10^{-2} and 4.3719×10^{-2}.

Table 1. The L_2 error and convergence order of spatial direction for $\beta = 0.3, 0.8$ at $t = 1$ with $\delta = (2 - \alpha_1)/\alpha_1$, $N = 1000$.

	h	L_2 error	Order
$\beta = 0.3$	3.1123e-1	2.8298e-04	—
	1.6759e-1	8.0832e-05	2.02
	8.6682e-2	1.8266e-05	2.25
	4.3719e-2	4.8952e-06	1.92
$\beta = 0.8$	3.1123e-1	3.2978e-04	—
	1.6759e-1	9.8644e-05	1.95
	8.6682e-2	2.4037e-05	2.14
	4.3719e-2	6.4715e-06	1.92

Example 5.2. Next, we consider the following fractional Bloch-Torrey equation on a circular domain

$$\begin{cases} l_1 \ {}_0^C D_t^{\alpha_1} u(x,y,t) + l_2 \, {}_0^C D_t^{\alpha_2} u(x,y,t) - \widetilde{k} \dfrac{\partial^{1+\beta} u(x,y,t)}{\partial |x|^{1+\beta}} - \widetilde{k} \dfrac{\partial^{1+\beta} u(x,y,t)}{\partial |y|^{1+\beta}} \\ = f(x,y,t), (x,y,t) \in \Omega \times (0,T], \\ u(x,y,0) = 0, \ (x,y) \in \overline{\Omega}, \\ u(x,y,t) = 0, \ (x,y,t) \in \partial\Omega \times (0,T], \end{cases}$$

Table 2. The L_2 error and convergence order of temporal direction for $\beta = 0.6$ at $t = 1$ with $h^2 = N^{-\min\{2-\alpha_1,\delta\alpha_1\}}$.

	N	h	L_2 error	Order
$\delta = \frac{2-\alpha_1}{2\alpha_1}$	28	3.1123e-1	3.0379e-04	—
	165	1.6759e-1	8.9439e-05	0.69
	1083	8.6682e-2	2.1089e-05	0.77
	7652	4.3719e-2	5.7561e-06	0.67
$\delta = \frac{1}{\alpha_1}$	10	3.1123e-1	3.0224e-04	—
	36	1.6759e-1	8.9517e-05	0.95
	133	8.6682e-2	2.1113e-05	1.10
	523	4.3719e-2	5.7515e-06	0.96

where $\Omega = \{(x,y)|x^2+y^2<1\}$, $T=1$,

$$
\begin{aligned}
f(x,y,t) &= \Big(l_1\Gamma(1+\alpha_1) + \frac{l_2\Gamma(1+\alpha_1)t^{\alpha_1-\alpha_2}}{\Gamma(1+\alpha_1-\alpha_2)}\Big)(x^2+y^2-1)^2 + \frac{\widetilde{k}t^{\alpha_1}}{2\cos(\pi(1+\beta)/2)}\\
&\Big[\Big(f_1(x,a_0,1+\beta)+g_1(x,b_0,1+\beta)\Big) + \Big(f_1(y,c_0,1+\beta)+g_1(y,d_0,1+\beta)\Big)\\
&+2(y^2-1)\Big(f_2(x,a_0,1+\beta)+g_2(x,b_0,1+\beta)\Big)\\
&+2(x^2-1)\Big(f_2(y,c_0,1+\beta)+g_2(y,d_0,1+\beta)\Big)\\
&+(y^2-1)^2\Big(f_3(x,a_0,1+\beta)+g_3(x,b_0,1+\beta)\Big)\\
&+(x^2-1)^2\Big(f_3(y,c_0,1+\beta)+g_3(y,d_0,1+\beta)\Big)\Big],
\end{aligned}
$$

$$
\begin{aligned}
&a_0 = -\sqrt{1-y^2},\ b_0 = \sqrt{1-y^2},\ c_0 = -\sqrt{1-x^2},\ d_0 = \sqrt{1-x^2},\\
&f_1(x,a,\beta) = {}_aD_x^\beta(x^4),\ f_2(x,a,\beta) = {}_aD_x^\beta(x^2),\ f_3(x,a,\beta) = {}_aD_x^\beta(1),\\
&g_1(x,b,\beta) = {}_xD_b^\beta(x^4),\ g_2(x,b,\beta) = {}_xD_b^\beta(x^2),\ g_3(x,b,\beta) = {}_xD_b^\beta(1).
\end{aligned}
$$

The exact solution is $u(x,y,t) = t^{\alpha_1}(x^2+y^2-1)^2$.

In this example, we take $\alpha_1 = 0.8$, $\alpha_2 = 0.7$, $l_1 = 1$, $l_2 = 0.5$, $\widetilde{k} = 1$. Fig.3 shows the circular domain partitioned by unstructured triangular meshes for different h. The corresponding numerical results are given in Table 3 and Table 4. By choosing different orders β, Table 3 illustrates the L_2 error and spatial convergence order with respect to varying mesh size h when taking $N = 1000$ and $\delta = (2-\alpha_1)/\alpha_1$. We can see that the convergence is of second order in the spatial direction. Table 4 displays the L_2 error and the convergence order of the temporal direction for $\beta = 0.6$ at $t = 1$ with $h^2 = N^{-\min\{2-\alpha_1,\delta\alpha_1\}}$. The orders of convergence displayed indicate that the rate of convergence is $N^{-\min\{2-\alpha_1,\delta\alpha_1\}}$, as predicted by Theorem 4.2. So the scheme and algorithm are also valid for the Bloch-Torrey equation with constant diffusion coefficient.

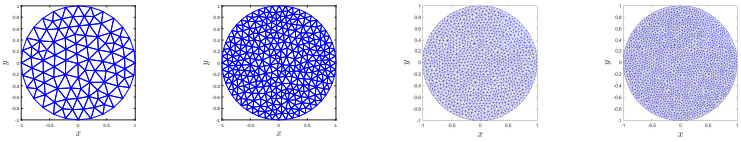

Fig. 3. The circular domain partitioned by unstructured meshes used in the calculation for $h \approx 2.8917 \times 10^{-1},\ 1.6444 \times 10^{-1},\ 8.6550 \times 10^{-2}$ and 7.1216×10^{-2}.

Table 3. The L_2 error and convergence order of spatial direction for $\beta = 0.3, 0.8$ at $t = 1$ with $\delta = (2-\alpha_1)/\alpha_1$, $N = 1000$.

	h	L_2 error	Order
$\beta = 0.3$	2.8917e-1	1.4428e-02	—
	1.6444e-1	4.0928e-03	2.23
	8.6550e-2	1.0137e-03	2.17
	7.1216e-2	6.4538e-04	2.32
$\beta = 0.8$	2.8917e-1	1.7611e-02	—
	1.6444e-1	5.4727e-03	2.07
	8.6550e-2	1.3908e-03	2.13
	7.1216e-2	9.0772e-04	2.18

Table 4. The L_2 error and convergence order of temporal direction for $\beta = 0.6$ at $t = 1$ with $h^2 = N^{-\min\{2-\alpha_1, \delta\alpha_1\}}$.

	N	h	L_2 error	Order
$\delta = \frac{2-\alpha_1}{2\alpha_1}$	63	2.8917e-1	1.6039e-02	—
	410	1.6444e-1	4.7804e-03	0.64
	3487	8.6550e-2	1.2127e-03	0.64
	6662	7.1216e-2	7.8324e-04	0.67
$\delta = \frac{2-\alpha_1}{\alpha_1}$	8	2.8917e-1	1.6429e-02	—
	20	1.6444e-1	4.8673e-03	1.32
	59	8.6550e-2	1.2124e-03	1.28
	82	7.1216e-2	7.8092e-04	1.34

Example 5.3. Finally, we consider the following fractional diffusion equation on an elliptical domain

$$\begin{cases} l_1\, {}_0^C D_t^{\alpha_1} u(x,y,t) + l_2\, {}_0^C D_t^{\alpha_2} u(x,y,t) - D_x\Big(k(x,y) D_{\theta_1}^{\beta} u(x,y,t)\Big) \\ -D_y\Big(k(x,y) D_{\theta_2}^{\beta} u(x,y,t)\Big) = f(x,y,t), \quad (x,y,t) \in \Omega \times (0,T], \\ u(x,y,0) = (4x^2 + y^2 - 1)^2, \ (x,y) \in \overline{\Omega}, \\ u(x,y,t) = 0, \ (x,y,t) \in \partial\Omega \times (0,T], \end{cases}$$

where $\Omega = \{(x,y)|4x^2+y^2<1\}$, $T=1$,

$$f(x,y,t) = \Big(\frac{l_1\Gamma(5)t^{4-\alpha_1}}{\Gamma(5-\alpha_1)} + \frac{l_2\Gamma(5)t^{4-\alpha_2}}{\Gamma(5-\alpha_2)}\Big)(4x^2+y^2-1)^2 - (1+t^4)\Big\{k_x(x,y)$$
$$\Big[\theta_1\Big(16f_1(x,a_0,\beta)+8(y^2-1)f_2(x,a_0,\beta)+(y^4-2y^2+1)f_3(x,a_0,\beta)\Big)$$
$$-(1-\theta_1)\Big(16g_1(x,b_0,\beta)+8(y^2-1)g_2(x,b_0,\beta)+(y^4-2y^2+1)g_3(x,b_0,\beta)\Big)\Big]$$
$$+k(x,y)\Big[\theta_1\Big(16f_1(x,a_0,1+\beta)+8(y^2-1)f_2(x,a_0,1+\beta)+(y^4-2y^2+1)$$
$$f_3(x,a_0,1+\beta)\Big)+(1-\theta_1)\Big(16g_1(x,b_0,1+\beta)+8(y^2-1)g_2(x,b_0,1+\beta)+$$
$$(y^4-2y^2+1)g_3(x,b_0,1+\beta)\Big)\Big]+k_y(x,y)\Big[\theta_2\Big(f_1(y,c_0,\beta)+2(4x^2-1)f_2(y,c_0,\beta)$$
$$+(16x^4-8x^2+1)f_3(y,c_0,\beta)\Big)-(1-\theta_2)\Big(g_1(y,d_0,\beta)+2(4x^2-1)g_2(y,d_0,\beta)$$
$$+(16x^4-8x^2+1)g_3(y,d_0,\beta)\Big)\Big]+k(x,y)\Big[\theta_2\Big(f_1(y,c_0,1+\beta)+2(4x^2-1)$$
$$f_2(y,c_0,1+\beta)+(16x^4-8x^2+1)f_3(y,c_0,1+\beta)\Big)+(1-\theta_2)\Big(g_1(y,d_0,1+\beta)$$
$$+2(4x^2-1)g_2(y,d_0,1+\beta)+(16x^4-8x^2+1)g_3(y,d_0,1+\beta)\Big)\Big]\Big\},$$
$$a_0=-\frac{1}{2}\sqrt{1-y^2},\ b_0=\frac{1}{2}\sqrt{1-y^2},\ c_0=-\sqrt{1-4x^2},\ d_0=\sqrt{1-4x^2},$$
$$f_1(x,a,\beta)={}_aD_x^\beta(x^4),\ f_2(x,a,\beta)={}_aD_x^\beta(x^2),\ f_3(x,a,\beta)={}_aD_x^\beta(1),$$
$$g_1(x,b,\beta)={}_xD_b^\beta(x^4),\ g_2(x,b,\beta)={}_xD_b^\beta(x^2),\ g_3(x,b,\beta)={}_xD_b^\beta(1).$$

The exact solution is $u(x,y,t)=(1+t^4)(4x^2+y^2-1)^2$.

In this test, we take $\alpha_1=0.8$, $\alpha_2=0.5$, $l_1=2, l_2=1$, $\theta_1=0.6$, $\theta_2=0.7$, $k(x,y)=x+y+100$. Fig.4 shows the elliptical domain partitioned by unstructured triangular meshes for different h. The time and space errors and convergence order are computed by choosing different values as shown in Table 5 and Table 6. The numerical results agree well with the convergence results in Theorem 4.2.

These numerical examples demonstrate that the proposed unstructured mesh finite element method is efficient in dealing with two-dimensional multi-term time and space fractional Bloch-Torrey equations with variable coefficients defined on a convex domains.

6. Conclusions

In this paper, we proposed an unstructured-mesh Galerkin finite element method for two-dimensional multi-term time and space fractional Bloch-Torrey equations

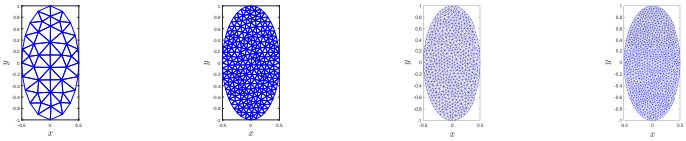

Fig. 4. The elliptical domain partitioned by unstructured meshes used in the calculation for $h \approx 3.0312 \times 10^{-1},\ 1.2558 \times 10^{-1},\ 8.3913 \times 10^{-2}$ and 6.9134×10^{-2}.

Table 5. The L_2 error and convergence order of spatial direction for $\beta = 0.3, 0.8$ at $t = 1$ with $\delta = (2 - \alpha_1)/\alpha_1$, $N = 1000$.

	h	L_2 error	Order
$\beta = 0.3$	3.0312e-1	8.4999e-02	—
	1.2558e-1	1.4043e-02	2.04
	8.3913e-2	5.2049e-03	2.46
	6.9134e-2	3.5241e-03	2.04
$\beta = 0.8$	3.0312e-1	9.1551e-02	—
	1.2558e-1	1.5465e-02	2.02
	8.3913e-2	5.8974e-03	2.39
	6.9134e-2	4.0081e-03	2.00

Table 6. The L_2 error and convergence order of temporal direction for $\beta = 0.6$ at $t = 1$ with $h^2 = N^{-\min\{2-\alpha_1, \delta\alpha_1\}}$.

	N	h	L_2 error	Order
$\delta = 1$	20	3.0312e-1	8.5849e-02	—
	179	1.2558e-1	1.4496e-02	0.81
	490	8.3913e-2	5.4420e-03	0.97
	796	6.9134e-2	3.7046e-03	0.87
$\delta = \frac{1}{\alpha_1}$	11	3.0312e-1	8.5824e-02	—
	63	1.2558e-1	1.4506e-02	1.02
	142	8.3913e-2	5.4471e-03	1.20
	209	6.9134e-2	3.7079e-03	1.00

with variable diffusivity coefficient on irregular convex domains. The L_1 method on graded meshes is used to approximate the temporal multi-term Caputo fractional derivative and FEM is used to discretise the space Riemann-Liouville fractional derivative. Also, the stability and convergence of the fully discrete scheme are discussed by presenting the error estimations with respect to the L^2 norm. Three numerical results demonstrated the versatility and application of the techniques.

Acknowledgements

This work was supported by the National Natural Science Foundation of China (Grant No. 11272024 and No. 11672011), the China Scholarship Council (CSC No. 201906020099) and the Australian Research Council via the Discovery Projects DP 180103858 and DP 190101889.

The authors would like to thank Dr. Libo Feng of Queensland University of Technology and Dr. Zongze Yang of Northwestern Polytechnical University for their valuable discussions on the topic.

References

1. F. Abdullah, F. Liu, P. Burrage, K. Burrage and T. Li, Novel analytical and numerical techniques for fractional temporal seir measles model, *Numer. Algorithms.* **79(1)** (2018) 19–40.
2. W. Bu, Y. Tang, Y. Wu and J. Yang, Finite difference/finite element method for two-dimensional space and time fractional Bloch-Torrey equations, *J. Comput. Phys.* **293** (2015) 264–279.
3. K. Burrage, N. Hale and D. Kay, An efficient implicit FEM scheme for fractional-in-space reaction-diffusion equations, *SIAM J. Sci. Comput.* **34(4)** (2012) A2145–A2172.
4. W. Deng, Finite element method for the space and time fractional Fokke-Planck equation, *SIAM J. Numer. Anal.* **47(1)** (2009) 204–226.
5. K. Diethelm, *The analysis of fractional differential equations: An application-oriented exposition using differential operators of Caputo type,* (Springer Science & Business Media, 2010).
6. B. Dumitru, D. Kai and S. Enrico, *Fractional Calculus: Models and Numerical Methods,* (World Scientific, 2012).
7. V. Ervin and J. Roop, Variational formulation for the stationary fractional advection dispersion equation, *Numer. Methods Partial Differ. Equ.* **22(3)** (2006) 558–576.
8. V. Ervin and J. Roop, Variational solution of fractional advection dispersion equations on bounded domains in $\mathbb{R}^d$, *Numer. Methods Partial Differ. Equ.* **23(2)** (2007) 256–281.
9. W. Fan, X. Jiang, F. Liu and V. Anh, The unstructured mesh finite element method for the two-dimensional multi-term time-space fractional diffusion-wave equation on an irregular convex domain, *J. Sci. Comput.* **77(1)** (2018) 27–52.
10. W. Fan, F. Liu, X. Jiang and I. Turner, A novel unstructured mesh finite element method for solving the time-space fractional wave equation on a two-dimensional irregular convex domain, *Fract. Calc. Appl. Anal.* **20(2)** (2017) 352–383.
11. L. Feng, P. Zhuang, F. Liu, I. Turner and Y. Gu, Finite element method for space-time fractional diffusion equation, *Numer. Algorithms.* **72(3)** (2016) 749–767.
12. L. Feng, F. Liu and I. Turner, Finite difference/finite element method for a novel 2D multi-term time-fractional mixed sub-diffusion and diffusion-wave equation on convex domains, *Commun. Nonlinear Sci. Numer. Simul.* **70** (2019) 354–371.
13. L. Feng, F. Liu, I. Turner, Q. Yang and P. Zhuang, Unstructured mesh finite difference/finite element method for the 2D time-space Riesz fractional diffusion equation on irregular convex domains, *Appl. Math. Model.* **59** (2018) 441–463.
14. Z. Hao, M. Park, G. Lin and Z. Cai, Finite element method for two-sided fractional differential equations with variable coefficients: Galerkin approach, *J. Sci. Comput.* **79(2)** (2019) 700–717.

15. C. Huang and M. Stynes, Superconvergence of a element method for the multi-term time-fractional diffusion problem, *J. Sci. Comput.* **82(1)** (2020) 10.
16. B. Jin, R. Lazarov and Z. Zhou, Error estimates for a semidiscrete finite element method for fractional order parabolic equations, *SIAM J. Numer. Anal.* **51(1)** (2013) 445–466.
17. A. Kilbas, H. Srivastava and J. Trujillo, *Theory and Applications of Fractional Differential Equations,* (Elsevier Science, 2006).
18. L. Li, F. Liu, L. Feng and I. Turner, A Galerkin finite element method for the modified distributed-order anomalous sub-diffusion equation, *J. Comput. Appl. Math.* **368** (2020) 112589.
19. Z. Lin, F. Liu, D. Wang and Y. Gu, Reproducing kernel particle method for two-dimensional time-space fractional diffusion equations in irregular domains, *Eng. Anal. Boundary Elem.* **97** (2018) 131–143.
20. F. Liu, V. Anh and I. Turner, Numerical solution of the space fractional Fokker-Planck equation, *J. Comput. Appl. Math.* **166(1)** (2004) 209–219.
21. F. Liu, P. Zhuang, V. Anh, I. Turner and K. Burrage, Stability and convergence of the difference methods for the space-time fractional advection-diffusion equation, *Appl. Math. Comput.* **191**, (2007), 12–20.
22. F. Liu, P. Zhuang, I. Turner, K. Burrage and V. Anh, A new fractional finite volume method for solving the fractional diffusion equation, *Appl. Math. Model.* **38**, (2014), 3871-3878.
23. F. Liu, P. Zhuang, I. Turner, V. Anh and K. Burrage, A semi-alternating direction method for a 2-D fractional FitzHugh-Nagumo monodomain model on an approximate irregular domain, *J. Comput. Phys.* **293**, (2015), 252–263.
24. F. Liu, P. Zhuang and Q. Liu, Numerical Methods of Fractional Partial Differential Equations and Applications, *Science Press*, China, (in Chinese), **November 2015** ISBN 978-7-03-046335-7.
25. F. Liu, L. Feng, V. Anh and J. Li, Unstructured-mesh Galerkin finite element method for the two-dimensional multi-term time-space fractional Bloch-Torrey equations on irregular convex domains, *Comput. Math. Appl.* **78(5)** (2019) 1637–1650.
26. L. Liu, L. Zheng, Y. Chen and F. Liu, Anomalous diffusion in comb model with fractional dual-phase-lag constitutive relation, *Comput. Math. Appl.* **76(2)** (2018) 245–256.
27. L. Liu, L. Zheng, F. Liu and X. Zhang, Anomalous convection diffusion and wave coupling transport of cells on comb frame with fractional Cattaneo-Christov flux, *Commun. Nonlinear Sci. Numer. Simul.* **38** (2016) 45–58.
28. L. Liu, L. Zheng, F. Liu and X. Zhang, Anomalous diffusion in finite length fingers comb frame with the effects of time and space riesz fractional cattaneo-christov flux and poiseuille flow, *J. Comput. Math.* **36(4)** (2018) 563–578.
29. Y. Liu, Z. Yu, H. Li, F. Liu and J. Wang, Time two-mesh algorithm combined with finite element method for time fractional water wave model, *Int. J. Heat Mass Tran.* **120** (2018) 1132–1145.
30. C. Ming, L. Zheng, X. Zhang, F. Liu and V. Anh, Flow and heat transfer of power-law fluid over a rotating disk with generalized diffusion, *Int. Commun. Heat Mass Tran.* **79** (2016) 81–88.
31. M. Paola, A. Pirrotta and A. Valenza, Visco-elastic behavior through fractional calculus: an easier method for best fitting experimental results, *Mech. Mater.* **43(12)** (2011) 799–806.
32. M. Pan, L. Zheng, F. Liu and X. Zhang, Modeling heat transport in nanofluids with stagnation point flow using fractional calculus, *Appl. Math. Model.* **40(21-22)** (2016)

8974–8984.

33. I. Podlubny, *Fractional Differential Equations: an Introduction to Fractional Derivatives, Fractional Differential Equations, to Methods of their Solution and some of their Applications,* (Elsevier, 1998).
34. S. Qin, F. Liu, I. Turner, V. Vegh, Q. Yu and Q. Yang, Multi-term time-fractional bloch equations and application in magnetic resonance imaging, *J. Comput. Appl. Math.* **319** (2017) 308–319.
35. S. Qin, F. Liu and I. Turner, A 2D multi-term time and space fractional bloch-torrey model based on bilinear rectangular finite elements, *Commun. Nonlinear Sci. Numer. Simul.* **56** (2018) 270–286.
36. S. Qin, F. Liu, I. Turner, Q. Yang and Q. Yu, Modelling anomalous diffusion using fractional Bloch-Torrey equations on approximate irregular domains, *Comput. Math. Appl.* **75(1)** (2018) 7–21.
37. H. Wang and D. Yang, Wellposedness of variable-coefficient conservative fractional elliptic differential equations, *SIAM J. Numer. Anal.* **51(2)** (2013) 1088–1107.
38. H. Wang, D. Yang and S. Zhu, Inhomogeneous dirichlet boundary-value problems of space-fractional diffusion equations and their finite element approximations, *SIAM J. Numer. Anal.* **52(3)** (2014) 1292–1310.
39. H. Wang, D. Yang and S. Zhu, A Petrov-Galerkin finite element method for variable-coefficient fractional diffusion equations, *Comput. Meth. Appl. Mech. Eng.* **290** (2015) 45–56.
40. H. Wang, D. Yang and S. Zhu, Accuracy of finite element methods for boundary-value problems of steady-state fractional diffusion equations, *J. Sci. Comput.* **70(1)** (2017) 429–449.
41. Z. Yang, Z. Yuan, Y. Nie, J. Wang, X. Zhu and F. Liu, Finite element method for nonlinear riesz space fractional diffusion equations on irregular domains, *J. Comput. Phys.* **330** (2017) 863–883.
42. Z. Yang, F. Liu, Y. Nie and I. Turner, An unstructured mesh finite difference/finite element method for the three-dimensional time-space fractional bloch- torrey equations on irregular domains, *J. Comput. Phys.* **408** (2020) 109284.
43. Q. Yu, F. Liu, I. Turner and K. Burrage, Numerical investigation of three types of space and time fractional bloch-torrey equations in 2D, *Open Physics.* **11(6)** (2013) 646–665.
44. Q. Yu, D. Reutens, K. OBrien and V. Vegh, Tissue microstructure features derived from anomalous diffusion measurements in magnetic resonance imaging, *Hum. brain mapp.* **38(2)** (2017) 1068–1081.
45. F, Zeng, C. Li, F. Liu and I. Turner, The use of finite difference/element approaches for solving the time-fractional subdiffusion equation, *SIAM J. Sci. Comput.* **35(6)** (2013) A2976–A3000.
46. F. Zeng, F. Liu, C. Li, K. Burrage, I. Turner and V. Anh, Crank-Nicolson ADI spectral method for the two-dimensional Riesz space fractional nonlinear reaction-diffusion equation, *SIAM J. Numer. Anal.* **52**, (2014), 2599-2622.
47. H. Zhang, F. Liu and V. Anh, Galerkin finite element approximation of symmetric space-fractional partial differential equations, *Appl. Math. Comput.* **217(6)** (2010) 2534–2545.
48. Y. Zhao, Y. Zhang, F. Liu, I. Turner and D. Shi, Analytical solution and nonconforming finite element approximation for the 2D multi-term fractional subdiffusion equation, *Appl. Math. Model.* **40(19-20)** (2016) 8810–8825.
49. P. Zhuang, F. Liu, V. Anh and I. Turner, New solution and analytical techniques of the implicit numerical methods for the anomalous sub-diffusion equation, *SIAM J.*

Numer. Anal. **46(2)**, (2008), 1079-1095.
50. P. Zhuang, F. Liu, V. Anh and I. Turner, Numerical methods for the variable-order fractional advection-diffusion with a nonlinear source term, *SIAM J. Numer. Anal.*, **47(3)**, (2009), 1760-1781.
51. M. Zheng, F. Liu, I. Turner and V. Anh, A novel high order space-time spectral method for the time-fractional Fokker-Planck equation, *SIAM J. Sci. Comput.* **37(2)**, (2015), A701-A724.
52. X. Zheng, V. Ervin and H. Wang, An indirect finite element method for variable-coefficient space-fractional diffusion equations and its optimal-order error estimates, *Commun. Appl. Math. Comput.* **2(1)** (2020) 147–162.